Theoretical study of the insulator/insulator interface: Band alignment at the SiO_2/HfO_2 junction

Onise Sharia,[1] Alexander A. Demkov,[1,*] Gennadi Bersuker,[2] and Byoung Hun Lee[2,†]
[1]*Department of Physics, The University of Texas at Austin, Austin, Texas 78712, USA*
[2]*SEMATECH, Austin, Texas 78741, USA*

(Received 17 August 2006; revised manuscript received 27 October 2006; published 5 January 2007)

While the physics of the Schottky barrier is relatively well understood, much less is known about the band alignment at the insulator/insulator interface. As a model problem we study theoretically the band alignment at the technologically important SiO_2/HfO_2 interface using density functional theory. We report several different atomic level models of this interface along with their energies and electronic properties. We find that the valence band offset increases near linearly with the interfacial oxygen coordination, changing from −2.0 eV to 1.0 eV. For the fully oxidized interface the Schottky limit is reached. We propose a simple model, which relates the screening properties of the interfacial layer to the band offset. Our results may explain a somewhat confusing picture provided by recent experiments.

DOI: 10.1103/PhysRevB.75.035306 PACS number(s): 73.40.Qv, 71.15.−m, 71.20.−b

I. INTRODUCTION

Theory of the band alignment at a heterojunction goes back over 60 years to Schottky.[1] The Schottky rule says that the discontinuity of the energy levels at the metal/semiconductor interface is a difference between the metal work function and electron affinity of the semiconductor. This simple recipe was so successful that most of the later theories provided just corrections to the so-called Schottky limit. Today the formation of the Schottky barrier at a metal/semiconductor interface is fairly well understood at the microscopic level,[2] and so is a band discontinuity between two semiconductors.[3] Conceptually, our understanding of the alignment at a metal-semiconductor junction is captured by the metal induced gap states (MIGS) theory.[4,5] The underlying physics is the charge transfer from the occupied metal states to empty evanescent states in the gap of a semiconductor resulting in a double layer with a corresponding interfacial dipole.[5,6] Tejedor and Flores[5] and Tersoff[3] used a similar approach for a junction between two semiconductors using a charge neutrality level (CNL) in analogy with the Fermi level. A CNL can be calculated from the complex band structure of a semiconductor or insulator.[7,8] Within the CNL approach, the first-order correction to the Schottky rule is simply the difference of two CNLs. Oxides are typically undoped (but can support fixed charges) so the Fermi level is not well defined, and it is not altogether clear whether concepts developed for metals and semiconductors still apply. From the historic perspective, the common anion rule[9,10] appears to be the most natural vehicle to estimate the band offset. Typically, the top of the oxide valence band is derived from the *p* states of oxygen (thus the common anion), and one would expect a small valence band offset. However, as we shall show, just as in the case of semiconductors[11,3] this simple argument breaks down. A predictive theory for the oxide/oxide interface is especially challenging, in part, due to the lack of knowledge of its atomic structure. Based on our microscopic models we propose a simple theory that relates the valence band offset to the average coordination of the interface oxygen. The correction to the Schottky rule can be separated into two effects: charge "spreading" across the interface originally discussed by Smoluchowsky,[12] which is qualitatively similar to the MIGS double layer, and screening of this charge by polarizable oxygen ions, which is the salient feature of our theory since it is pertinent mostly to ionic oxide materials.

The band alignment at the oxide/oxide interface has recently become technologically important because of its role in the advanced complementary metal oxide semiconductor (CMOS) technology. The gate stack in a metal oxide semiconductor (MOS) transistor works as a capacitor. The stack capacitance defines the transistor threshold voltage and saturation current passing through the device, which are its major performance characteristics. With scaling of the transistor gate length, the capacitance needs to be increased in order to maintain control over the threshold voltage. This can be achieved by decreasing the thickness of a gate dielectric. However, as the thickness of the currently used SiO_2 dielectric can no longer be reduced because of high gate leakage (a parasitic current caused by direct quantum tunneling), an increase of capacitance can only be obtained by using high dielectric constant (high-*k*) materials such as, e.g., HfO_2, ZrO_2, or Al_2O_3. Hafnium-based dielectrics, like hafnium dioxide and hafnium silicates, are the leading candidates for replacing silicon dioxide as a gate dielectric. These materials can be deposited by several techniques: atomic layer deposition (ALD), metal-organic chemical-vapor deposition (MOCVD), PVD, using various precursors.[13] However, in all cases, a thin SiO_2 layer, grown either intentionally or spontaneously, is present at the interface between the high-*k* film and Si substrate after standard fabrication processing is completed. The band offset between SiO_2 and HfO_2 is unknown but clearly determines the overall alignment of the gate stack. It is possible that our failure to correctly include the dipole layer at the oxide-oxide interface contributes to our inability to explain many experimental results in these advanced gate stacks.[14]

In this paper we report a theoretical study the SiO_2/HfO_2 interface using the density functional theory. We have constructed several atomistic models which differ by the interfacial oxygen coordination, HfO_2 phases and strain. We use these structures to calculate the band discontinuity, thus relating the microscopic structure of the stack to its electric

TABLE I. Lattice constants for bulk hafnia.

	Theoretical	Experimental[a]
Cubic		
V (Å^3)	30.82	32.77
a (Å)	4.98	5.08
Tetragonal		
V (Å^3)	31.29	34.66
a (Å)	4.97	5.14
c (Å)	5.06	5.25
δ_z	0.043	
Monoclinic		
V (Å^3)	32	34.58
a (Å)	5.013	5.117
b (Å)	5.117	5.175
c (Å)	5.1753	5.291
β	99.406°	99.22°

[a]Reference 18.

properties. The analysis of trends thus computed allows us to put forward the aforesaid model of the band alignment. The rest of the paper is organized as follows. We briefly describe computational procedures used in this work in Sec. II. We describe several interface models and simple rules for their construction in Sec. III. In Sec. IV we discuss our calculations of the band discontinuity.

II. COMPUTATIONAL METHOD

Ab initio density functional theory (DFT) calculations are performed using a pseudopotential plane wave basis code VASP.[15] We use the local density approximation (LDA). For most of the calculations Vanderbilt-type ultrasoft pseudopotentials are used. We have compared these results with those obtained using the projected augmented wave (PAW) method, which is also used to generate the site projected densities of states. The PAW method is computationally as fast as pseudopotential methods but has an accuracy approaching that of the full potential augmented plane wave method.[16] The kinetic energy cutoff of 600 eV is used, along with the $8\times8\times8$ k-point mesh for the integration over the Brillouin zone. For bulk SiO_2 and HfO_2 this affords convergence up to 10^{-4} eV/cell. The calculated value of the lattice constant for β-cristobalite (the so-called C9 structure) SiO_2 is 7.34 Å, or 2.5% larger than the experimental value.[17] The lattice constants along with the internal atomic coordinates for cubic, tetragonal, and monoclinic polymorphs of hafnia are summarized in Table I. For tetragonal hafnia we start with $\delta=0.025$ and experiential lattice constants.[18] For a fixed value of a we optimize c, and relax the atomic positions. Then we optimize a for the best found c. We repeat this process once again starting with our already optimized lattice constants to get a better precision. The same full optimization was done for the monoclinic structure.

To study the silica/hafnia interface we build atomic level models in supercell and slab geometry with cell sizes ranging from $5.19\times5.19\times29.31$ Å^3 to $5.19\times5.19\times49.60$ Å^3. We use a $4\times4\times1$ k-point mesh centered at the Gamma point. Increasing the number of k points to $8\times8\times2$ results in 0.01 eV/cell change in the total energy, which is an order of magnitude less than the energy differences we are concerned with in this paper. The change in the average electrostatic potential is less than 0.02 eV thus the band offset estimate is converged at a one percent level with respect to the Brillouin zone integration.

III. ATOMIC STRUCTURE OF THE SiO_2/HfO_2 INTERFACE

When building a theoretical model for a hafnia-silica interface three issues need to be considered. First, the lattice mismatch needs to be accommodated by strain; second, there is a "metal" coordination mismatch between the two oxides, and third the so called electron counting rule needs to be satisfied. The lattice constants of crystalline silica and hafnia differ by 4% (theoretical number), and one needs to decide which oxide should be considered a substrate, and which the epitaxial film. The film is then strained to conform to the size of the substrate. Silicon forms tetrahedral bonds typical of sp^3-hybrids, while $3d$-electrons of hafnium determine its high-coordination (7 or 8). Thus there is a coordination mismatch at the oxide-oxide interface. Alternatively, one may consider oxygen coordination in two oxides. Depending on the polymorph, oxygen in HfO_2 is three- or fourfold coordinated. In SiO_2, the structure of which is a (4,2)-net, oxygen is twofold coordinated. Of course, in experiment, silica is actually amorphous [a classic example of a continuous random network (CRN)]. However, the coordination mismatch to hafnia is the same for the crystalline and amorphous phases. Nature obviously forms a transition layer but the mismatch creates difficulties in building a theoretical interface model. For example, in the case of cubic HfO_2 each layer in the (001) direction has four oxygen atoms per metal atom, while in β-cristobalite it is two. So if there are common oxygen atoms in the interfacial plane it is impossible to fully satisfy both hafnia and silica. Another difficulty is that the interface has to be insulating. Robertson has used simple electron counting arguments to build interfaces which satisfy this condition.[19]

As stated above, the layer of silica on which hafnia is subsequently grown is amorphous, while hafnia is crystalline. Hafnia appears to be amorphous as deposited,[20] but crystallizes upon the so-called postdeposition densification anneal (600 °C) since the crystallization temperature is only 350 °C.[21] Both amorphous and crystalline silica share the (4,2)-net structure, therefore we consider a crystal/crystal interface thus effectively reducing the problem to epitaxy. Since our main interest is the band alignment we hope that this simplification still allows us to capture the essential physics of the problem.

A. Interfaces with cubic hafnia

We build interfaces between β-cristobalite SiO_2 and cubic and monoclinic polymorphs of HfO_2. We start with the case

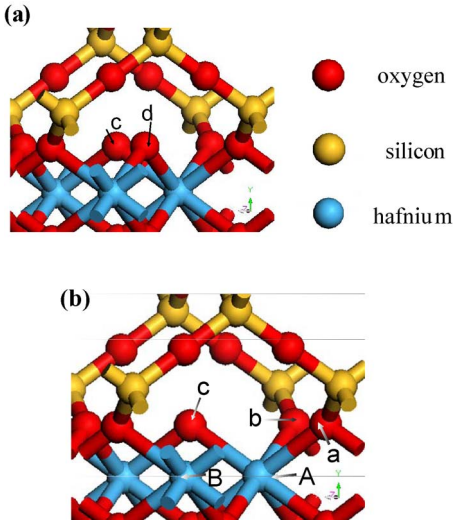

FIG. 1. (Color online) Unrelaxed atomic structure of the interface between β-cristobalite and cubic hafnia. To keep the structure insulating one oxygen atom needs to be removed. (a) The structure before removing an oxygen atom. (b) The structure after removing an oxygen atom.

of cubic hafnia. Instead of a conventional cubic cell of β-cristobalite we choose a smaller body-centered tetragonal (bct) cell which is rotated 45 degrees in the horizontal plane with respect to a conventional cell (the starting structure is still cubic rather than $\bar{I}42d$ for we keep $\frac{c}{a}=1$). Lattice constants for this cell are $a=b=\frac{7.34}{\sqrt{2}}=5.19$ Å and $c=7.34$ Å. The mismatch between this cell and cubic HfO_2 is 4%. We assume silica to be a "substrate," and consider HfO_2 to be under tensile strain to match SiO_2. The interface before relaxation is shown in Fig. 1(a). If we do not remove one oxygen atom from the interface the system is metallic. Each oxygen atom needs two electrons to fill its shell, and each hafnium has four electrons (thus the 2:1 stoichiometry of the oxide). In Fig. 1(b) we have removed one oxygen atom [labeled d in Fig. 1(a)] from the interface. Note that since there are two interfaces in the supercell, we can choose a "symmetric" removal scheme when d is removed on both sides and "asymmetric" one when different oxygen atoms are removed. We first discuss the asymmetric case. The interface hafnium atom A is bonded to four fourfold coordinated oxygen atoms in hafnia, two bridge oxygen atoms (labeled a and b), and to one two-fold interface oxygen atom (labeled c). A

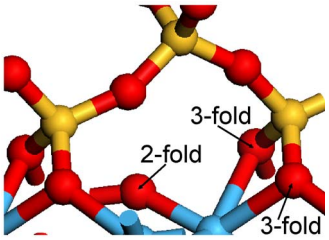

FIG. 2. (Color online) The interface of Fig. 1 after the relaxation is shown. We find two threefold coordinated bridge oxygen atoms and one twofold interface oxygen atom. We call this interface c-332.

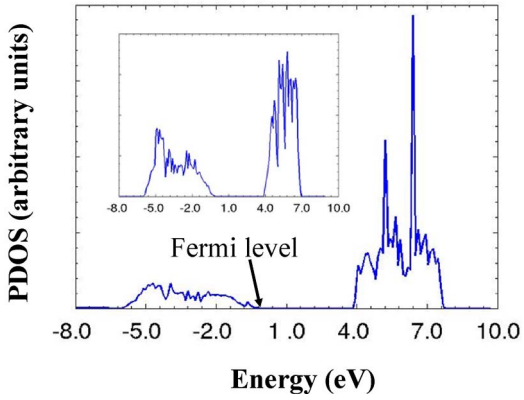

FIG. 3. (Color online) The partial density of states (DOS) projected on the d orbital of hafnium in the "bulk" hafnia region of the supercell of the c-332 interface. The d-orbital hafnium-projected DOS of bulk m-HfO_2 is shown in the inset for comparison.

bridge oxygen atom is connected to two hafnium atoms and one silicon atom. Thus hafnium A gives each bridge oxygen atom $\frac{1}{2}$ of an electron (one electron total). Fourfold oxygen atoms in hafnia get 1/2 of an electron each (two electrons total). If the twofold interface oxygen receives one electron from atom A the electron counting is satisfied (in other words all bonds are saturated). The same is true for hafnium atom B.

The first supercell consists of 12 layers (22 Å) of silica and 6 layers (15.6 Å) of hafnia (12:6 cell). We relax atomic positions with the conjugate gradient method. Figure 2 shows the interface of Fig. 1 after the relaxation; it has two threefold bridge oxygen atoms and one twofold interface oxygen atom. We call this interface c-332. HfO_2 is not truly cubic anymore; we see sevenfold hafnium atoms, as well as threefold and fourfold oxygen atoms. This local geometry is similar to that found in monoclinic hafnia. Another argument for this is the electronic density of states (DOS). In Fig. 3 we show the DOS projected on the hafnia region of the supercell; the DOS of m-HfO_2 is shown in the insert for comparison. Note the absence of the characteristic splitting of the d states in the bottom of the conduction band. The change in the structure of hafnia also causes a distortion in the structure of SiO_2. Hafnia expands, and because of its larger elastic constants, it does so at the expense of silica. A slight complication comes from the fact that C9 is not the lowest energy structure of cristobalite.[22] By changing the size of the hafnia-occupied portion of the cell in the direction normal to the interface while keeping the lateral dimensions fixed and optimizing all internal coordinates we find that for the 12:6

TABLE II. Interfacial bonding information for the c-332 interface.

	Si-O-Hf	Hf-O-Hf
Si-O distance (Å)	1.60	
Hf-O distance (Å)	2.42	1.94–1.97
Angle	91.60°	144.46°

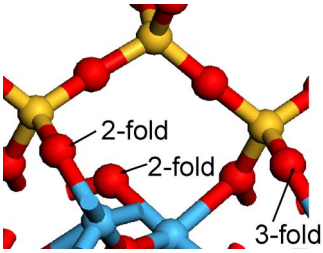

FIG. 4. (Color online) The c-322 SiO_2/HfO_2 interface after the relaxation; the bonding information for the interfacial atoms is given in Table III.

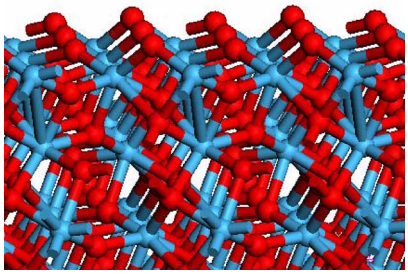

FIG. 5. (Color online) The structure of the relaxed (001) surface of monoclinic hafnia. The number of oxygen atoms at the surface is adjusted to ensure the slab is stoichiometric and the surface insulating.

SiO_2/HfO_2 supercell $c=37.59$ Å results in a strain free C9 cristobalite. The resulting c-332 structure used for the band offset calculations is shown in Fig. 2. The bonding information for the interfacial atoms is given in Table II.

In addition to the c-332 interface model we have found another metastable structure with a notably different bonding arrangement. It is 0.9 eV/cell higher in energy than the c-332 structure (this is equivalent to a 535 erg/cm^2 difference in the interface energy). We start with a "symmetric" removal of oxygen, and repeat the relaxation procedure. Again $c=37.59$ Å results in a strain free silica. However, the interface bonding appears quite different. In Fig. 4 we see one threefold oxygen and two twofold oxygen atoms, one similar to a twofold oxygen atom at the c-332 interface, and one in a bridging Si-O-Hf position. We label this interface c-322. The bonding information for the interfacial atoms is given in Table III.

Cubic and tetragonal phases of hafnia are thermodynamically stable only at very high temperature, and only the monoclinic phase is stable at room temperature. To do a more realistic calculation we consider four interfaces with monoclinic hafnia.

B. Interfaces with monoclinic hafnia

When considering high symmetry structures, the simplest way to comply with the periodic boundary conditions dictated by supercell geometry is to have both interfaces in the cell identical. In the case of a low symmetry structure this, however, severely limits the number of possible interfaces one can construct for a given cell size. In the case of monoclinic hafnia (m-HfO_2) the only interface we are able to construct is m-332. After the relaxation it remains m-332. The monoclinic structure of the film did not change (the atomic positions adjust by less than 0.01 Å). To investigate other possibilities we switch to using slab geometry instead. Technically this amounts to adding a vacuum layer on top of HfO_2 and relaxing the atomic positions. A vacuum layer also simplifies the strain relaxation procedure (unfortunately VASP does not support the constant pressure dynamics). If the system is strained laterally it is now allowed to relax in the normal direction.

We build three types of interfaces, m-332, m-322, and m-222; as before the numeric index refers to the oxygen coordination at the interface. The structures are made of ten layers of silica (18.4 Å) and eight layers of hafnia (19.3 Å). The thickness of the vacuum layer separating hafnia from silica is 11.9 Å, and the overall thickness of the simulation cell is 49.60 Å. The (001) SiO_2 surface initially Si terminated is saturated with hydrogen. The (001) surface of hafnia is free and special care has been taken to keep the overall structure insulating. We show this surface structure in Fig. 5. To match the monoclinic hafnia cell to β-cristobalite it has been strained in the following way. As a starting point we use the structure of fully optimized monoclinic HfO_2 (space group $P2_1/c$). The lattice parameters are $a=5.01$ Å, $b=5.12$ Å, $c=5.17$ Å, and $\beta=99.41°$. We strain a and b to match the 5.19 Å of silica (3.6% and 1.4% strain) and relax β and c to minimize the energy, we find $\beta=100.86°$ and $c=5.08$ Å. Repeating these strained m-HfO_2 cells four times along the lattice vector $\vec{c}$ allows a near perfect match to β-cristobalite, the matching is shown in Fig. 6. As a result there is no strain (or relaxation) in the SiO_2 portion of the cell. Hafnia maintained its original monoclinic structure almost as well as silica. Three relaxed structures are shown in Fig. 7. All three structures appear to be stable with the exception of m-222 where a minor re-adjustment occurs in the second hafnia layer. The bonding information for all three interfaces is summarized in Table IV. Three cells contain the same number of atoms and differ only in the interface geometry. The total energy of m-332 is 0.7 eV less then m-322

TABLE III. Interfacial bonding information for the c-322 interface.

	Si-O-Hf (two-fold oxygen)	Si-O-Hf (three-fold oxygen)	Hf-O-Hf
Si-O distance (Å)	1.61	1.63	
Hf-O distance (Å)	1.93	2.09	1.92–1.94
Angle	145.55°	117.38°	123.53°

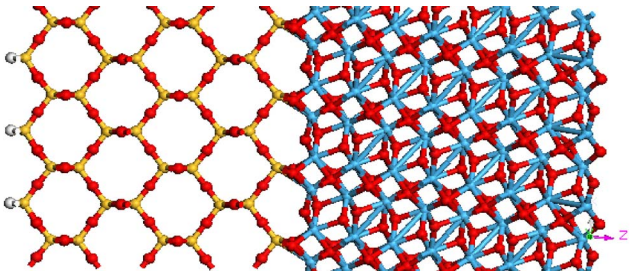

FIG. 6. (Color online) A slab model of the interface between monoclinic hafnia and β-cristobalite. The silica surface is hydrogen terminated. The number of oxygen atoms on the free hafnia surface is adjusted to eliminate gap states (same as in Fig. 5). The vacuum layer is 10 Å thick.

and 1.5 eV less then m-222. So as in the cubic case, we find the larger the number of metal-oxygen bonds results in lower interface energy.

C. Terminal oxygen at the interface

Our next interface is shown in Fig. 8. There is one terminal oxygen atom at the interface. The super-cell contains seven layers of silica and seven layers of hafnia, the total thickness of the simulation cell is 29.31 Å. The electron count rule is satisfied, and hafnia remains cubic after the relaxation. In addition to the terminal oxygen, there are two twofold coordinated bridging oxygen atoms at the interface, and we call this model c-221. The terminal Hf-O bond is 1.74 Å. Bridging oxygen atoms form 1.61 Å long bonds to Si and 1.87 Å long bonds to Hf. The Si-O-Hf bond angle is 175.7°.

To examine the possible effect of the system size we perform calculations with a smaller cell comprised of eight layers of silica and five layers of cubic hafnia, and a larger one with twelve layers of silica and nine layers of hafnia (both "asymmetric," hafnia is strained to match silica). The interface relaxes into a c-322 structure with the same bonding pattern as a larger cell.

IV. BAND ALIGNMENT AT THE SiO_2/HfO_2 INTERFACE

To estimate the conduction band offset between two insulators we start with the Schottky limit, which is simply the difference between two electron affinities, and in our case is 1.6 eV (we use the experimental value of 2.5 eV and 0.9 eV for electron affinities of hafnia and silica, respectively[23]). However, since we use a DFT-LDA method, only the valence band discontinuity can be calculated, therefore from now on we will discuss the valence band offset (VBO), unless it is specified otherwise. Incidentally, the VBO is also 1.6 eV in the Schottky limit. Alternatively, in the strong pinning or Bardeen limit for the silica interface with c-hafnia we obtain a VBO of 2.4 eV, and for the interface with m-hafnia we obtain a VBO of 1.3 eV (we use charge neutrality levels of silica and hafnia from 24). In general, within the MIGS theory one could expect values between the Schottky and Bardeen limits. However, our *ab initio* calculations show that the offset may differ significantly from that predicted in either limit.

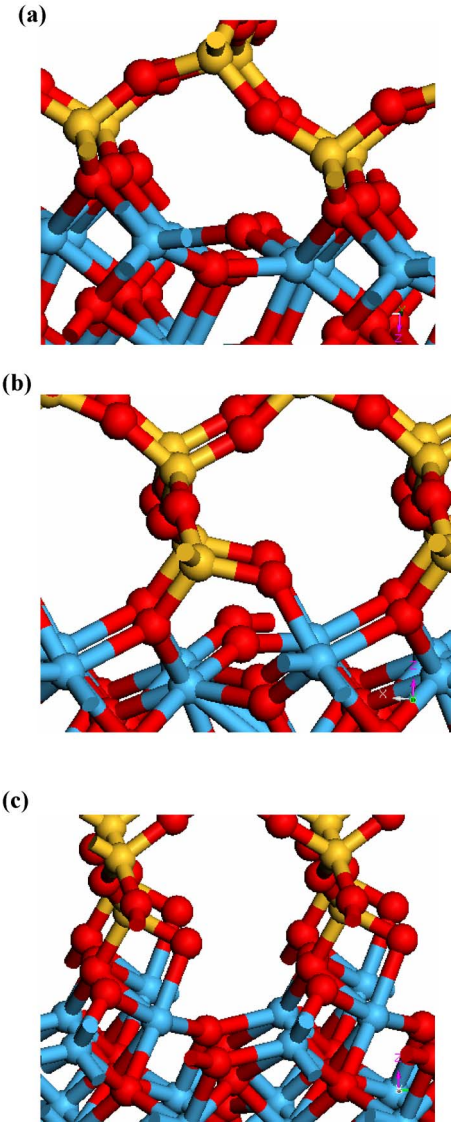

FIG. 7. (Color online) Relaxed structures of the interface between monoclinic hafnia and β-cristobalite with different coordination of the interfacial oxygen: (a) m-332 structure, (b) m-322 structure, and (c) m-222 structure. Strictly speaking, the m-222 structure actually has one three-fold oxygen atom but one bond is broken in the second hafnia layer and we consider it effectively 222.

To calculate the VBO at the SiO_2/HfO_2 interface we use two methods. The first one is the reference potential method originally introduced by Kleinman.[25] As reference energy we use the macroscopically averaged electrostatic potential as proposed by Van de Walle and Martin.[26] The method requires two additional bulk calculations of silica and hafnia to locate the valence band top (VBT) in each material with respect to the average potential. For a supercell (or a slab) containing the interface we calculate the average potential using the formula

TABLE IV. Bonding information for interfaces with monoclinic hafnia.

	Si-O-Hf (two-fold oxygen)	Si-O-Hf (three-fold oxygen)	Hf-O-Hf
m-332			
Si-O distance (Å)		1.63	
Hf-O distance (Å)		2.1–2.25	1.95
Angle		100.75°–111.92°	149.53°
m-322			
Si-O distance (Å)	1.60	1.67	
Hf-O distance (Å)	1.99	2.13–2.22	1.93–2.01
Angle	129.16°	111.16°	111.16–129.16°
m-222			
Si-O distance (Å)	1.61–1.68		
Hf-O distance (Å)	1.99–2.12		1.90–2.02
Angle	98.29°		117.22°

$$\bar{V}(z) = \frac{1}{d_1 d_2} \int_{z-d_1/2}^{z+d_1/2} dz' \int_{z'-d_2/2}^{z'+d_2/2} dz'' V(z''),$$

where $V(z)$ is the xy-plane averaged potential and d_1 and d_2 are the interplanar distances along the z direction (normal to the interface) in silica and hafnia, respectively.[27] This produces a smooth potential as shown in Fig. 9 for the c-221 structure. Assuming that far away from the interface the potential reaches its bulk value one can place corresponding VBTs with respect to the average potential on both sides of the interface using the bulk reference, and thus determine the VBO. The second method is more direct, and is based on the analysis of the site projected partial density of states. As in many oxides, the valence band top in silica and hafnia is derived mainly from the oxygen p states. If the simulation cell is big enough, so that the density of states does not change within a few layers deep inside the region occupied by silica or hafnia, we can identify the edge of the oxygen p-state density of states with the bulk VBT, and thus determine the offset. The strength of the reference potential method is its fast convergence with the cell size. However, the density of states analysis in our case shows reasonable convergence as well because of the large oxide band gaps.

We have three interfaces of silica with cubic hafnia. Unfortunately, in most cases the cubic structure of hafnia is distorted and we cannot use the value of the average potential from the bulk c-HfO_2 as a reference. Instead we use the site projected density of states method. We find the valence band offsets of 0.9 eV and 0.2 eV for the interfaces c-332 and c -322, respectively. The offset appears to be governed by the interfacial oxygen coordination. As we will show this is a fundamental property of this interface. The c-221 cell of hafnia, which contains terminal oxygen, maintains its cubic structure and we use the reference potential method. The analysis is shown in Fig. 9; the VBO is −1.9 eV. Note that the valence band top of hafnia is now below that of silica.

For the monoclinic structures in slab geometry we again find the VBO of 0.9, 0.2, and −0.7 eV for m-332, m-322, and

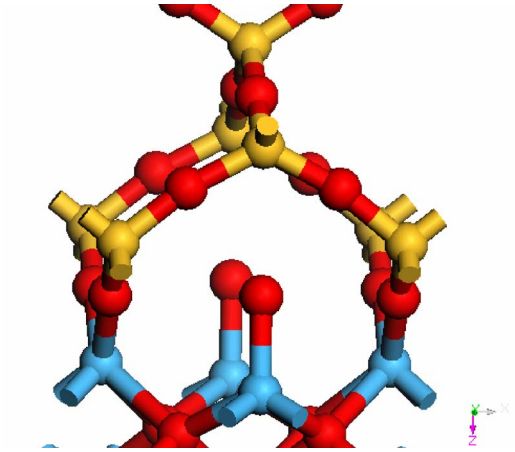

FIG. 8. (Color online) The interface of c-HfO_2 with β-cristobalite containing a terminal oxygen atom. We call this interface c-221.

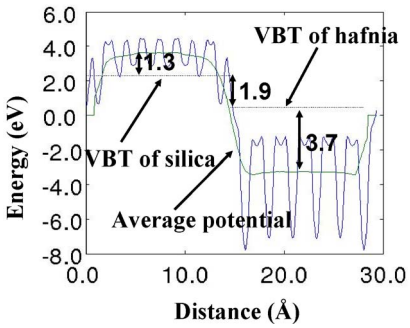

FIG. 9. (Color online) The planar-averaged and macroscopic average (smooth line) electrostatic potential for the c-221 SiO_2/HfO_2 interface (supercell geometry). Using two separate bulk calculations we place the valence band top on each side of the interface with respect to the average potential, and thus determine the valence band offset of 1.9 eV.

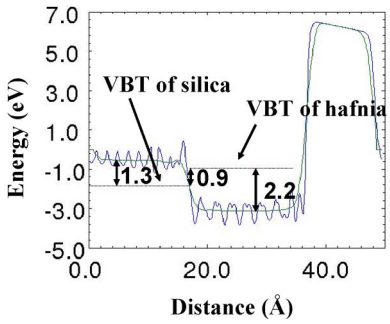

FIG. 10. (Color online) The planar-averaged and macroscopic average (smooth line) electrostatic potential for the m-332 SiO_2/HfO_2 interface (slab geometry). Using the same method as in Fig. 9 the valence band offset of 0.9 eV is found. A weak electric field can be seen in the vacuum region, its contribution to the offset is insignificant and therefore neglected.

m-222 structures, respectively. For the m-332 interface we show the reference potential method results in Fig. 10 and the site projected density of states analysis in Fig. 11, the close agreement between two methods is reassuring. We also perform a calculation for the m-332 structure using supercell geometry and still find the offset of 1.0 eV. The 0.1 eV difference is within the typical accuracy of these calculations.[28] Results of our VBO calculations for all structures are summarized in Table V. Regardless of the starting phase of hafnia, the cell choice, or the calculation setup (a slab vs a supercell) the valence band offset is about 1.0 eV for structures with highly coordinated interfacial oxygen, very small for the intermediate cases and negative for poorly coordinated interfaces. We now plot the calculated band offset as a function of the interfacial oxygen coordination (see Fig. 12). It is clear that as the average coordination of the interface oxygen increases the Schottky limit is recovered.

To understand this peculiar behavior let us start from the very beginning. (i) Before the oxides are brought into contact the band discontinuity is given by the Schottky rule. (ii)

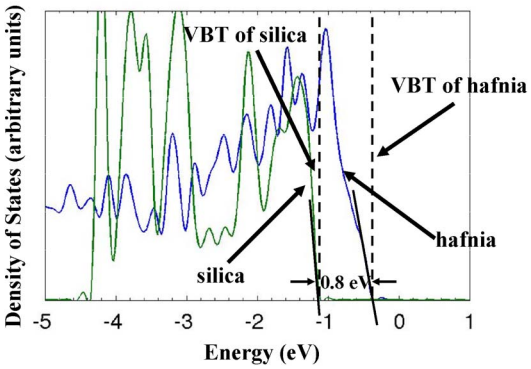

FIG. 11. (Color online) The site projected partial density of states method for the band offset at the m-332 SiO_2/HfO_2 interface. The DOS is projected onto p orbitals of oxygen atoms deep in the bulk regions of silica and hafnia. The valence band offset is determined as a difference between the edges (determined by tangents at the density's tail) and is 0.8 eV, in good agreement with the reference potential method.

TABLE V. Valence band offsets for different interfaces.

SiO_2/HfO_2 interface	Δ_{VBO} (eV) (reference potential method)	Δ_{VBO} (eV) (site projected DOS method)
c-332		0.9
c-322		0.2
c-221	−1.9	−2.1
m-332 (slab)	0.9	0.8
m-332 (supercell)	1.0	0.9
m-322	0.2	0.1
m-222	−0.7	−0.5

When the oxides are brought together the charge transfer becomes possible, and a correction needs to be added. The top of the valence band in hafnia is at higher energy than that in silica before the contact, so the charge transfer would be from hafnia to silica. The valence electron density should undergo a smooth transition from the hafnia value of $0.476\frac{e}{Å^3}$ (we use the volume of the strained cell) to that in silica $\left(0.324\frac{e}{Å^3}\right)$ as required by the kinetic energy term in the Hamiltonian. This transfer would result in the "depletion" at the hafnia side and "accumulation" at the silica side or in formation of a double layer with the field pointing toward silica. In the case of a metal surface Smoluchowsky called this effect "spreading."[12] Alternatively, the interface dipole can be seen as associated with the difference in the charge neutrality levels of the two insulators.[5] "Locally" the charge transfer may be thought of in terms of the difference in the electronegativity of metals[29] (1.3 and 1.9 for Hf and Si, respectively) which ultimately defines the CNLs. Regardless of the specific model a dipole layer would form across the 2–4 Å of the interface (compare with $d_{SiO}+d_{HfO}=3.6$ Å) and shift the Schottky answer. Note that all our interfaces connect silica to hafnia through a common oxygen plane. In Fig. 13 we show the average macroscopic charge density for m-322 and c-221 structures in the direction normal to the interface. The corresponding average bulk electron density is subtracted on both sides of the interface. As expected, hafnia is charged positively and silica negatively. Formation of a

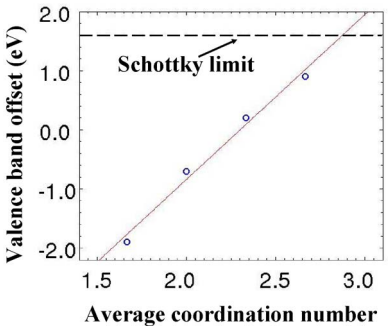

FIG. 12. (Color online) The valence band offset for several structures plotted as a function of the average coordination of the interfacial oxygen. Dashed line corresponds to Schottky limit recovered for a hypothetical interface with all oxygen threefold coordinated.

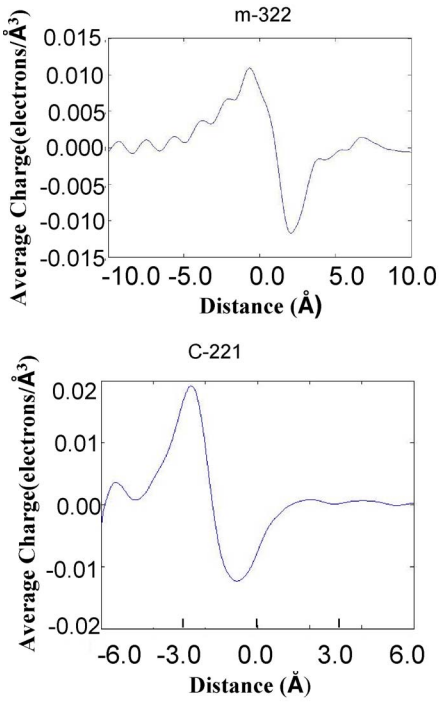

FIG. 13. (Color online) The interface dipole for the m-322 and c-221 SiO_2/HfO_2 interfaces. First the average charge density is subtracted from the each side of the interface (0.32 and 0.48 electrons/Å^3 for silica hafnia, respectively). The actual shape of the dipole is sensitive to the choice of the interfacial plane which is not clearly defined. Our choice results in the symmetric charge spit. The dipole corresponding to the c-221 interface is about twice that for the m-322 interface, resulting in a larger correction to the Schottky limit.

double layer due to the charge "spreading" is the basis of the MIGS theory. Note that the charge density difference between silica and hafnia is eight times larger than that between Si and let us say Al. Thus the situation is different and more complicated in the case of oxides. (iii) Interfacial oxygen atoms are polarizable and can move in response to the internal field set by the double layer. In Fig. 14 we show the dipole layer (charge density difference) for the m-332 structure before and after oxygen atoms are allowed to relax. Clearly, the dipole is reduced after the relaxation. The induced oxygen polarization reduces the internal field in the dipole layer caused by the "spreading," and moves the offset back to the Schottky limit. In other words one can think of the problem in terms of first charging a planar capacitor and then inserting a "dielectric," which is of course just a layer of the interfacial oxygen. And the dielectric constant of this "dielectric" is a function of the average oxygen coordination. Note that this is principally different from interlayers commonly used to tune the band alignment at a semiconductor/semiconductor interface via control over the Fermi level pinning.[30]

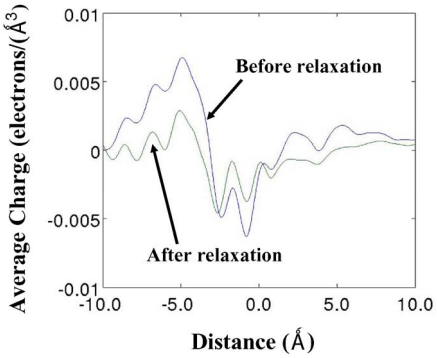

FIG. 14. (Color online) The interface dipole for m-332 SiO_2/HfO_2 interface before and after the interface oxygen relaxes. The dipole is larger before the relaxation indicating the screening role of oxygen.

Approximating the double layer with a plane capacitor we can estimate a correction to the Schottky rule. The surface charge density is given simply by

$$\sigma = \frac{\bar{\rho} d}{2},$$

where $2d$ is the thickness of the interface layer (we take $d = 1.4$ Å, approximately the distance between two atomic planes), $\bar{\rho}$ is half of the difference between two densities or 0.076 electrons/Å^3. Then the potential drop across the interfacial layer is

$$\Delta V = \frac{\bar{\rho} d^2}{2\varepsilon_0 \varepsilon}.$$

Here ε is the dielectric response of the interfacial layer. Thus for the total band offset we have

$$V_{vb} = V_{\text{Schottky}} - \frac{\bar{\rho} d^2}{2\varepsilon_0 \varepsilon} = 1.6 - \frac{13.5}{\varepsilon}\ (\text{eV}).$$

In Fig. 15(a) we show the dielectric constant as a function of the oxygen coordination backed out from the *ab initio* result (Fig. 12) using this expression. It varies smoothly form the silica-like to hafnia-like value [4 (Ref. 31) and 22 (Ref. 32), respectively] as we go from twofold to threefold interface. Considering that the electronic component is small (2 for silica,[33] and 5 for hafnia[34]) we attribute the coordination dependence of the dielectric constant to the lattice polarizability. The latter can depend on the local geometry (bonding) either through the vibrational mode frequency ω_λ or through the Born effective charge $\tilde{Z}^*_{\lambda\alpha}$:

$$\varepsilon^{\text{lattice}}_{\alpha\beta} = \frac{4\pi e^2}{MV} \sum_\lambda \frac{\tilde{Z}^*_{\lambda\alpha} \tilde{Z}^*_{\lambda\beta}}{\omega^2_\lambda}.$$

We assign the dependence to the Born effective charge. Assuming the average ε_∞ of 3.5 and fitting the value of Z^* for $N_{\text{average}}=3$ we use a crude approximation $\varepsilon_{\text{lattice}} = \beta(Z^*_{N_{\text{avearge}}})^2$ and extract the oxygen Born effective charge as a function of its average coordination [see Fig. 15(b)]. The values are quite reasonable, for example, for the twofold coordinated oxygen in bulk SiO_2 Gonze *et al.* report the Born effective charge (spherically averaged) of −1.6,[35] while for the fourfold coordinated oxygen in cubic and tetragonal hafnia Vanderbilt reports $Z^* = -2.9$, with similar values for the monoclinic polymorph.[36] We are currently exploring the

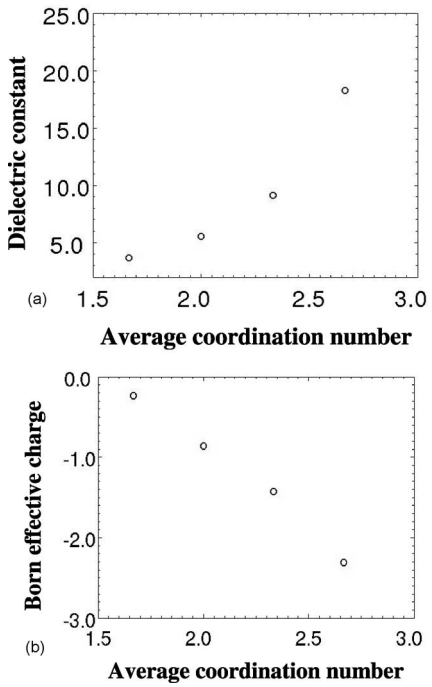

FIG. 15. (a) The effective dielectric constant of the SiO_2/HfO_2 interface as a function of the average interfacial oxygen coordination backed out of the *ab initio* result (shown in Fig. 12) using a simple capacitor model (see text). (b) The Born effective charge for the interface oxygen as a function of its average coordination based on (a) (see text).

relation of the dielectric constant to the atomic coordination in more details.

Let us now examine how these results relate to experiment. A study of the HfO_2-SiO_2-Si gate stack was performed by Sayan, Emge, Garfunkel, and co-workers using a combination of x-ray and inverse photoemission and *ab initio* theory,[37] and the Zr-ZrO_2-SiO_2-Si system was investigated by Fulton, Lucovsky, and Nemanich employing x-ray and ultraviolet photoemission spectroscopy.[38] From Fig. 5 in Ref. 32 we infer the SiO_2/HfO_2 valence band offset to be between 0.89 and 1.25 eV depending on the method of analysis, while Fulton *et al.* report the SiO_2/ZrO_2 valence band offset of 0.67 ± 0.24 eV. Both values are in qualitative agreement with our findings and seem to indicate a reasonably good interface with the average oxygen coordination of 2.5.

V. CONCLUSIONS

In this paper we report on a study of the SiO_2/HfO_2 interface using density functional theory. The valence band offset is found to vary between −2.0 eV and 1.0 eV depending on the microscopic structure of the interface, and to depend strongly on the average coordination of the interface oxygen. The Schottky limit value of 1.6 eV is expected to be recovered for the fully oxidized interface. We suggest that the correction to the Schottky limit has two sources. First, the charge transfer across the interface ("spreading") lowers hafnia states and raises those of silica resulting in a dipolar shift. Second, the subsequent polarization of the interfacial oxygen atoms in response to the dipole layer's field reduces the dipolar shift. The final band offset value is mostly determined by the interface layer polarizability. A simple empirical model is proposed that relates the band offset to the microscopic structure of the interface. Our results agree well with the available experiment. Most importantly, they highlight the significance of the SiO_2/HfO_2 interface in the high-k dielectric gate stacks engineering. Moreover, the coordination of the interfacial oxygen is most likely determined during the initial ALD deposition cycle, pointing to the importance of the deposition conditions and quality of the starting silica surface. It also depends on the thermal budget of the fabrication process that may cause re-arrangement of the interface bonds. The lower oxygen coordination results in a smaller VBO but a larger conduction band offset. This dependence on the process conditions may explain the variation in experimental data.

*Electronic mail: demkov@physics.utexas.edu
†IBM assignee.

[1] W. Schottky, Z. Phys. **118**, 539 (1942).
[2] M. Peressi, N. Binggeli, and A. Baldereschi, J. Phys. D **31**, 1273 (1998).
[3] J. Tersoff, Phys. Rev. Lett. **56**, 2755 (1986).
[4] C. Tejedor and F. Flores, J. Phys. C **11**, L19 (1978).
[5] S. Louie and M. Cohen, Phys. Rev. B **13**, 2461 (1976).
[6] J. Bardeen, Phys. Rev. **71**, 717 (1947).
[7] V. Heine, Phys. Rev. **138**, A1689 (1965).
[8] J. A. Appelbaum and D. R. Hamann, Phys. Rev. B **10**, 4973 (1974).
[9] O. McCaldin, T. C. McGill, and C. A. Mead, Phys. Rev. Lett. **36**, 56 (1976).
[10] W. R. Frensley and H. Kroemer, Phys. Rev. B **16**, 2642 (1977).
[11] W. A. Harrison, J. Vac. Sci. Technol. **14**, 1016 (1977).
[12] R. Smoluchowsky, Phys. Rev. **60**, 661 (1941).
[13] M. Ritala, M. A. Leskelä, L. Niinisto, T. Prohaska, G. Friedbacher, and M. Grasserbauer, Thin Solid Films **250**, 72 (1994); P. Kirsch *et al.*, J. Appl. Phys. 99, 023508 (2006).
[14] R. Chau, IEEE Electron Device Lett. **25**, 408 (2004).
[15] G. Kresse and F. Furthmuller, Phys. Rev. B **54**, 11169 (1996); G. Kresese and J. Futhmuller, Comput. Mater. Sci. **6**, 15 (1996); G. Kresse and J. Hafner, Phys. Rev. B **47**, RC558 (1993); **48**, 13115 (1993); **49**, 14251 (1994); J. Phys.: Condens. Matter **6**, 8245 (1994).
[16] P. Blöchl, Phys. Rev. B **50**, 17953 (1998).
[17] R. W. G. Wyckoff, *Crystal Structures* (Wiley, New York, London, 1965).
[18] J. Wang, H. P. Li, and R. Stevens, J. Mater. Sci. **27**, 5397 (1992).
[19] P. W. Peacock and J. Robertson, Phys. Rev. Lett. **92**, 057601 (2004).

[20] D. Triyoso, R. Liu, D. Roan, M. Ramon, N. V. Edwards, R. Gregory, D. Werho, J. Kulik, G. Tam, E. Irwin, X.-D. Wang, L. B. La, C. Hobbs, R. Garcia, J. Baker, B. E. White, Jr., and P. Tobin, J. Electrochem. Soc. **151**, F220 (2004).
[21] S. V. Ushakov, A. Navrotsky, Y. Yang, S. Stemmer, K. Kukli, M. Ritala, M. A. Leskelä, P. Fejes, A. A. Demkov, C. Wang, B.-Y. Nguyen, D. Triyoso, and P. Tobin, Phys. Status Solidi B **241**, 2268 (2004).
[22] A. A. Demkov, J. Ortega, M. P. Grumbach, and O. F. Sankey, Phys. Rev. B **52**, 1618 (1995).
[23] J. Robertson, J. Non-Cryst. Solids **303**, 94 (2002).
[24] A. A. Demkov, L. R. C. Fonseca, E. Verret, J. Tomfohr, and O. F. Sankey, Phys. Rev. B **71**, 195306 (2005).
[25] D. M. Bylander and L. Kleinman, Phys. Rev. B **36**, 3229 (1987).
[26] C. G. Van de Walle and R. M. Martin, Phys. Rev. B **39**, 1871 (1989).
[27] C. G. Van de Walle and R. M. Martin, Phys. Rev. B **35**, 8154 (1987).
[28] A. A. Demkov, Phys. Rev. B **74**, 085310 (2006).
[29] R. T. Tung, Phys. Rev. Lett. **84**, 6078 (2000).
[30] A. D. Katnani, P. Chiaradia, Y. Cho, P. Mahowald, P. Pianetta, and R. S. Bouer, Phys. Rev. B **32**, 4071 (1985).
[31] S. M. Sze, *Physics of Semiconductor Devices* (Wiley, New York, 1981).
[32] M. Balog, M. Schieber, M. Michman, and S. Patai, Thin Solid Films **41**, 247 (1977).
[33] L. E. Ramos, J. Furthmuller, and F. Bechsted, Phys. Rev. B **69**, 085102 (2004).
[34] G.-M. Rignanese, X. Gonze, G. Jun, K. Cho, and A. Pasquarello, Phys. Rev. B **69**, 184301 (2004).
[35] X. Gonze, D. C. Allan, and M. P. Teter, Phys. Rev. Lett. **68**, 3603 (1992).
[36] X. Zhao and D. Vanderbilt, Phys. Rev. B **65**, 233106 (2002).
[37] S. Sayan, T. Emge, E. Garfunkel, X. Zhao, L. Wielunski, R. A. Bartynski, D. Vanderbilt, J. S. Suehle, S. Suzer, and M. Banszak-Holl, J. Appl. Phys. **96**, 7485 (2004).
[38] C. C. Fulton, G. Lucovsky, and R. J. Nemanich, J. Appl. Phys. **99**, 063708 (2006).